Production of ^{15}O for Medical Applications via the $^{16}O(\gamma,n)^{15}O$ Reaction

Stacy L. Queern[1,2], Ryan Cardman[3], Christopher S. Loveless[1,2], Matthew R. Shepherd[3], and Suzanne E. Lapi[1,2]

[1]Department of Radiology, University of Alabama at Birmingham, Birmingham, Alabama; [2]Department of Chemistry, Washington University in St. Louis, St. Louis, Missouri; and [3]Department of Physics, Indiana University, Bloomington, Indiana

^{15}O (half-life, 122 s) is a useful radionuclide for PET applications. Current production of ^{15}O typically makes use of the $^{14}N(d,n)^{15}O$, $^{15}N(p,n)^{15}O$, or $^{16}O(p,pn)^{15}O$ reactions using an accelerator. A novel approach for the production of ^{15}O is via the $^{16}O(\gamma,n)^{15}O$ reaction using an electron linear accelerator. Photonuclear reactions using an electron linear accelerator may allow for feasible and economical production of ^{15}O compared with the current methods. **Methods:** In this work, experiments using a repurposed Clinac were conducted using oxygen-containing alumina as a target material to study the production rate of ^{15}O. Additional studies were conducted using a water target cell. Simulations using Geant4 were conducted to predict the activity and power dissipation in the target. **Results:** Bremsstrahlung radiation from the electron beam, and consequently ^{15}O production via photonuclear reactions, is enhanced when a high-*Z* material, tungsten, is placed in front of the target. The alumina irradiations provided preliminary data to optimize the beam parameters and target configuration. The optimal thickness of tungsten was 1.4 mm for both the simulated and the measured studies of alumina. Simulations of irradiated water targets showed that tungsten thicker than 1.4 mm resulted in fewer photons available to activate the water; thus, a higher current was required to achieve a fixed dose. Alternatively, for a constant tungsten thickness, more power was deposited in the target with increasing beam energy, requiring a lower current to achieve a fixed dose. Actual irradiations of a water target yielded a quantity of ^{15}O in the water that was consistent with expectations based on irradiations of alumina. **Conclusion:** Several parameters should be considered regarding the photonuclear production of ^{15}O for an average patient dose of 1,850 MBq (50 mCi) in 10 mL. This work illustrates a variety of machine parameters capable of achieving a reasonable patient dose. Our simulations show that the power deposited in the target for these parameters is less than that in commercially operated cyclotron targets for the production of ^{18}F. Thus, this work demonstrates that the photonuclear production of ^{15}O may be a new production path for this useful radionuclide.

Key Words: molecular imaging; radiochemistry; oxygen-15; positron emission tomography; eLINAC; photonuclear

J Nucl Med 2019; 60:424–428
DOI: 10.2967/jnumed.118.215681

The radionuclide ^{15}O is a positron emitter with a half-life of 122.24 s. The versatility and simplicity of the chemical forms of ^{15}O (^{15}O-O_2, ^{15}O-CO, ^{15}O-CO_2, and, perhaps most importantly, ^{15}O-H_2O) combined with its large fraction of positron decay have led to numerous uses in PET imaging research (*1–3*). It has been used for applications in neurology, cardiology, and oncology to evaluate oxygen consumption, lung perfusion, blood distribution, blood flow, and myocardial perfusion using ^{15}O-H_2O (*1–5*). Current means for the production of ^{15}O typically require a proton or deuteron accelerator, with the most common pathway of production being via the $^{14}N(d,n)^{15}O$ reaction using a nitrogen gas target and producing ^{15}O in the form of ^{15}O-O_2 or ^{15}O-H_2O (*1,3,4*). Production of ^{15}O with protons has also been described using the reactions $^{15}N(p,n)^{15}O$ or $^{16}O(p,pn)^{15}O$ (*1,4*). For various applications, ^{15}O can be converted to ^{15}O-CO or other forms with rapid, online gas-phase chemistry.

A novel approach for the production of ^{15}O is via the $^{16}O(\gamma,n)^{15}O$ reaction using an electron linear accelerator (eLINAC). Photonuclear reactions using an eLINAC may allow for low-cost ^{15}O production compared with the current methods (*6–8*). The eLINAC method induces nuclear reactions (typically (γ,n) or (γ,p)) using bremsstrahlung radiation produced from high-energy electrons incident on a high-*Z* material (*6,7,9*). Conceptually, this route may allow for nearly direct use of the bombarded material after irradiation. The bolus could also be piped to a PET/CT installation some distance from the eLINAC or transported by a pneumatic transfer system.

The excitation function for the $^{16}O(\gamma,n)^{15}O$ reaction shown in Figure 1 illustrates an optimal energy range for production using 20- to 30-MeV photons to make use of the largest production cross-section of ^{15}O while considering the power deposition in the target. Electron energies of greater than 30 MeV are required to produce photons in the range of 20–30 MeV via bremsstrahlung radiation.

Herein we report on initial studies investigating yield and the feasibility of production of ^{15}O via the photonuclear route. Initial simulations and experiments were conducted using alumina as an oxygen-containing target material to determine optimal machine settings and to inform target design. After these experiments, additional irradiation studies were conducted using a water target cell. Simulations of ^{15}O production with different configurations of a water cell, different converter thicknesses, and varying beam energies were conducted.

MATERIALS AND METHODS

Materials

Tungsten was purchased from Midwest Tungsten Service with a thickness of 0.28 mm, alumina was purchased from McMaster-Carr

Received Jun. 7, 2018; revision accepted Sep. 5, 2018.
For correspondence or reprints contact: Suzanne E. Lapi, Department of Radiology, University of Alabama at Birmingham, 1824 6th Ave. S., WTI 310F, Birmingham, AL 35294.
E-mail: lapi@uab.edu
Published online Sep. 20, 2018.

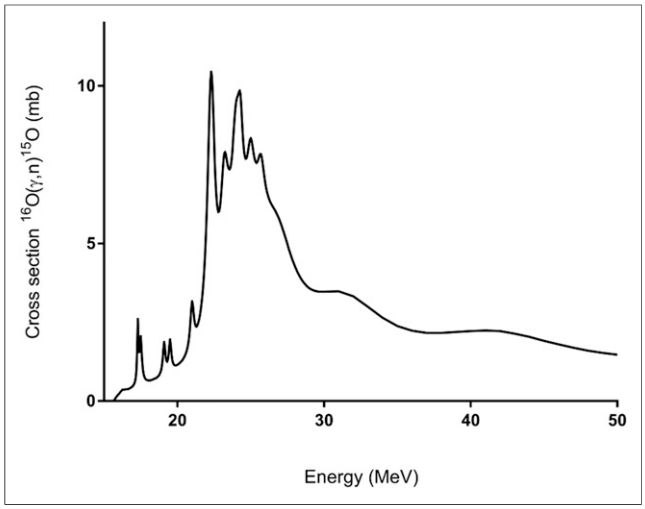

FIGURE 1. Excitation function for $^{16}O(\gamma,n)^{15}O$ (*12–13*).

with a thickness of 3 mm and a density of 2.0 g/cm^3, and glass shell vials were purchased from Fisher Scientific. All materials were machined locally at Indiana University's machine shop. Tungsten and alumina were cut into 1.27-cm squares.

Instrumentation

A Clinac (2100; Varian) was used for all irradiations. The target holder and targets were produced at the Indiana University onsite machine shop. A target holder was fabricated such that it mated to fixtures used for holding beam-shaping filters inside the machine. This design allowed for the placement of target materials very near the exit aperture of the accelerator. Therefore, the full electron beam current was directed onto a millimeter-sized spot on the target, permitting a much larger beam flux on target than if target materials were placed at the machine iso-center, where radiotherapy patients are typically placed. Our system implemented a high-*Z* material (tungsten) as an electron converter, which enhances the production of photons via bremsstrahlung radiation as the electrons interact with the converter. Various thicknesses of tungsten were examined. The average current of the machine, which has a pulsed-beam structure, was calibrated using an open-air alternating current transformer fabricated by Bergoz Instrumentation and mounted in the same location as the target holder.

After irradiation, each target was measured using a calibrated high-purity germanium detector (Canberra) and the data were analyzed to determine the amount of ^{15}O produced. For each spectrum, it was assumed that the annihilation photons from the positrons from ^{15}O decay are the only contributor to the 511-keV peak. The 511-keV peaks were integrated and corrected for decay during acquisition to determine the activity at the start of the acquisition. Multiple acquisitions were collected in series on the same sample. The activity at the start of the acquisition was then plotted against the time since beam off and fit to an exponential decay function with 2 parameters: half-life and activity at beam off.

As we were limited to maximum beam currents of about 5 μA and electron beam energies of 22 MeV, we relied on computer simulations to explore machine configurations that are beyond these limits and better suited for efficient ^{15}O production. A computer model of the target geometry and material was constructed in the Geant4 simulation framework (*10–12*). The Geant4 code was then used to track the propagation of the electron beam and the subsequent production of bremsstrahlung photons in the target material. The bremsstrahlung spectrum and photon pathlength in the material, as simulated by Geant4, was then used to calculate the ^{15}O activity using the cross-section depicted in Figure 1.

Production of ^{15}O in Alumina

Initial simulations and experiments were conducted using alumina (Al_2O_3) in the form of ceramic tiles as an oxygen-containing target material. Alumina offered many beneficial features for these preliminary studies, such as the similarity between the oxygen nuclear density of alumina (3.54×10^{19} oxygen atoms/mm^3) and water (3.34×10^{19} oxygen atoms/mm^3). Alumina also has good machinability, and low activation for other byproducts to be produced via photonuclear routes, allowing for the alumina to provide a workable proxy for a water target.

Several irradiations were completed using alumina to investigate the activity produced with varying tungsten converter thicknesses. The different thicknesses studied for the converter included 0.84, 1.4, 1.68, 1.96, 2.24, 2.52, and 3.64 mm. Corresponding simulations of similar target geometries and beam properties were conducted to validate aspects of the simulation using the experimentally determined activity.

Production of ^{15}O in Water

Three different cylindric water targets were used in the simulations with 3 different volumes as shown in Figure 2. These configurations provided different material depths, different radii, and different volumes to be investigated. Each of these targets was simulated with electron beam energy of 22, 25, 30, and 40 MeV and an electron current of 0.5 μA. These simulations were completed to calculate the activity produced and power dissipation in each target for 5-min irradiations. Target 1 was used in further simulations with varying converter thicknesses of 1.4, 4, 7, and 10 mm and electron energies of 25, 30, and 40 MeV, with the current being adjusted to give a final ^{15}O yield of 1,850 MBq (50 mCi). Thus, these experiments determined the current required to obtain a fixed activity for various converters and the activity per power dissipation relationship as a function of converter thickness.

After the simulations, irradiations were conducted using a water target to verify the yields of ^{15}O produced compared with alumina and to determine whether the produced ^{15}O remained in the water. A small glass cell was constructed with a 12.7-mm diameter and 4.4-mm length holding a volume of 0.5 mL of water. Several irradiations were completed with the water target using a converter thickness of 1.4 mm and a duration of 5 min. After irradiation, the cell was opened and the irradiated water was transferred to a new vial for measurement to omit activated oxygen in the glass vial itself.

RESULTS

Production of ^{15}O in Alumina

Figure 3 shows the Geant4 simulation results and the measured irradiated alumina for ^{15}O. Although this figure shows that the

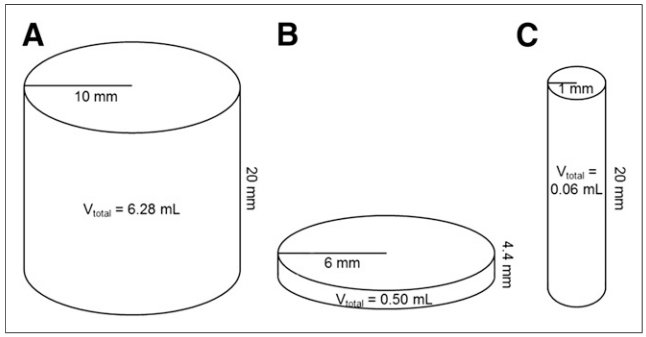

FIGURE 2. Water target configurations for the Geant4 simulations.

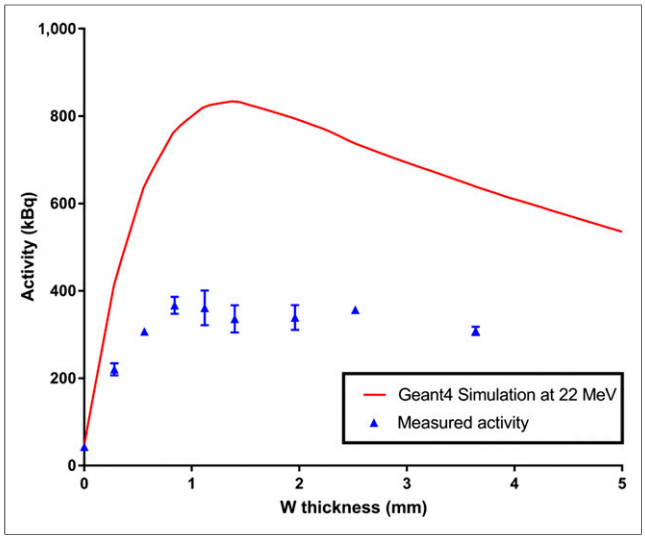

FIGURE 3. Measured and calculated activity vs. tungsten thickness for alumina.

simulations disagreed by about a factor of 2 compared with the measured activity, the trend illustrates that a converter thickness of 1.4 mm for both the simulated and the measured studies yields the maximum produced activity. This trend can be understood as follows. Initially, increasing the converter thickness enhances the bremsstrahlung radiation, and hence activity, as expected. However, as the thickness is further increased, absorption of radiated high-energy photons begins to become significant and flux reaching the target is diminished, thereby reducing the activity for thicker converters. These competing effects generate an optimum thickness for maximum activity, which appears to be accurately predicted by the simulation. There are systematic uncertainties in both predicting and measuring the absolute activity: cross section (*13,14*), distribution of energy of beam particles, stability of the machine current, conversion efficiency of emitted positrons, and subsequent detection efficiency of 511-keV photons. These systematic uncertainties almost completely cancel in measuring ratios of activities, giving confidence in our ability to predict relative activity between various target configurations and hence optimize the target geometry. A systematic uncertainty about the prediction of absolute activity at the level of a factor of 2 is sufficient to assess the feasibly of this production route.

Production of ^{15}O in Water

Simulations of the 3 target configurations from Figure 2 are shown in Figure 4 for each water target. The simulation for each target used a 1.4-mm-thick tungsten converter and a 0.5-μA current for a 5-min irradiation, and the electron beam energy was varied with energies of 22, 25, 30, and 40 MeV. The simulation showed target 1 to have the most relevant working profile because of the reasonable volume (6.28 mL) and larger activity produced; therefore, further simulations were conducted with this target. The studies with alumina indicated an optimal converter thickness to maximize activity. However, in the case of a water target, one may also be interested in minimizing target heating to reduce the practical challenge of avoiding target boiling. Although activity is produced by high-energy bremsstrahlung photons, target heating tends to be dominated by the more copious low-energy electrons and positrons produced in the interaction with the converter. As the target thickness is increased, the components of the electromagnetic shower that produce mainly heating are absorbed at a different rate than those that produce activity, leading to a variation of activity per unit energy deposited in the target. To explore this dependence, we simulated other thicknesses beyond that which produced maximum activity. Converters less than 1.4 mm thick yielded both reduced activity and a larger power dissipation in the target than those at 1.4 mm and, hence, appeared to have no practical advantage in either enhancing produced activity or reducing thermal load on the target. For each simulation, the simulated duration of irradiation was 5 min while the current was adjusted to yield an end-of-irradiation radioactivity of 1,850 MBq (50 mCi). The beam energy was varied with energies of 25, 30, and 40 MeV. Table 1 displays these calculations for different converter thicknesses.

Several trends can be seen in Table 1. As a thicker converter (>1.4 mm) is used, an increased current is required to obtain the desired 1,850 MBq (50 mCi), but less power is deposited in the target. As the beam energy increases for the same converter thickness, a lower current is required to achieve 1,850 MBq (50 mCi). It should be noted that, for a specific converter thickness and beam energy, the values in the table (required beam current, power dissipation in target, and total beam power) scale directly for different amounts of radioactivity by multiplying the ratio of radioactivity of interest to the radioactivity used in the Table (1,850 MBq). Simulations using Geant4 yielded a maximum power dissipation in the target of 200.6 W for a current of 63.3 μA and a 25-MeV beam energy to produce 1,850 MBq (50 mCi). For reference, the power dissipation for a proton beam in a typical ^{18}O-H_2O target to produce ^{18}F is 900 W for a current of 50 μA and an 18-MeV beam energy. This is much higher than the photonuclear reaction power dissipation. Thus, cooling strategies are available for the proposed water target for photonuclear ^{15}O production

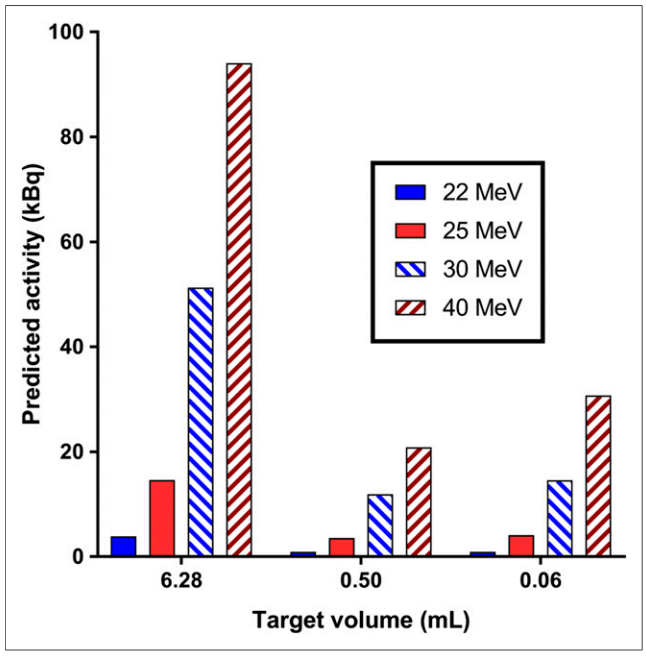

FIGURE 4. Amount of predicted activity produced in the target for several water target geometries.

TABLE 1
Geant4 Simulations for the Target 1 Water Configuration to Produce 1,850 MBq (50 mCi) in 5 Minutes with Varying Parameters

Converter thickness (mm)	Simulated beam energy (MeV)	Required beam current (μA)	Power dissipation in target (W)	Total beam power (W)
1.4	25.0	63.3	200.7	1,583
	30.0	18.0	63.1	541
	40.0	9.8	38.5	393
4.0	25.0	81.3	49.5	2,032
	30.0	22.8	23.2	685
	40.0	9.2	16.7	393
7.0	25.0	118.0	23.7	2,950
	30.0	34.0	9.9	1019
	40.0	13.5	7.7	366
10.0	25.0	170.0	21.9	4,249
	30.0	52.3	10.2	1568
	40.0	20.3	7.1	542

based on previous work for similar volumes for high-power ^{18}F production water targets (*15,16*).

Five-minute experimental irradiations of the water cell were conducted using a 1.4-mm tungsten converter with 22-MeV beam energy and a 0.5-μA current. The series of activity measurements as a function of time since beam off was fit to an exponential decay curve as seen in Figure 5. These results illustrate that the half-life of our produced radioactivity matches the half-life of ^{15}O. The produced amount is comparable to that produced in alumina studies, which used a material with a similar oxygen atom density and geometry. This finding indicates that the bulk of the activated oxygen remains in the water.

DISCUSSION

The simulated activity of alumina targets for different converter thicknesses allowed for converter thickness to be optimized, producing the maximum amount of activity. The alumina irradiations with the Clinac allowed for the activity to be measured and for the optimal converter configuration to be determined. The optimal converter thickness for this configuration both simulated and experimentally was found to be 1.4 mm of tungsten, validating the ability of the simulation as a tool to optimize target geometry.

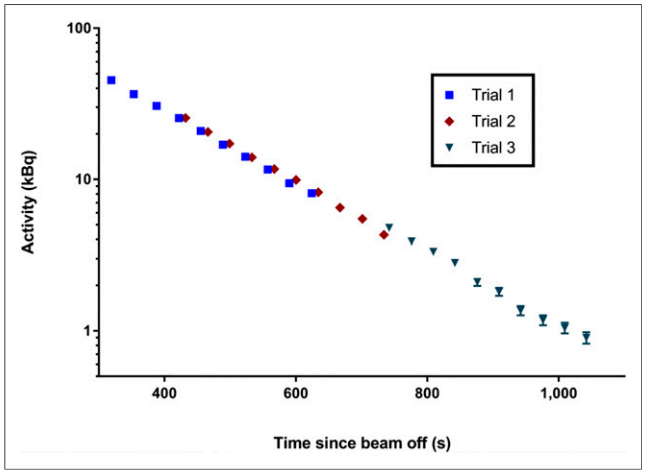

FIGURE 5. Measured activity of the ^{15}O from the water target.

Although measurements and simulation deviated somewhat on absolute quantity of activity, good agreement was achieved with respect to relative activity, indicating that the simulations provide a guide to the expected trends of power deposition and activity as a function of tungsten converter thickness. Geant4 simulations illustrated that significant amounts of ^{15}O were achievable using photon-induced nuclear reactions with the available eLINAC and allow for calculations of what parameters would be required to produce clinically useful amounts. The measured water target irradiations show that the ^{15}O produced was radionuclidically pure, with measurable amounts of activity that allow extrapolation to patient doses.

Several parameters for the photonuclear production of ^{15}O in water should be considered to optimize the production of patient doses. An average patient dose is 1,850 MBq (50 mCi) in a volume of 10 mL diluted in saline (*17*), and hence Table 1 indicates a variety of configurations that all produce a 1,850-MBq (50 mCi) dose in the target 1 geometry, which appears to have a reasonable volume and shape. Two trends are evident in Table 1. First, for a fixed converter thickness, increasing the beam energy decreases the total beam power required to achieve fixed activity. Second, for a fixed beam energy, increasing the converter thickness (>1.4 mm) decreases the power dissipation in the target but increases the total beam power requirement to achieve a fixed activity. An optimal configuration is likely to depend on engineering considerations that place constraints on the beam energy, beam power, or power dissipation in target. The specifications of existing commercial targets indicate that the power dissipation in the target for the photonuclear reactions is such that the required cooling for the proposed photonuclear targets should be achievable. Although the threshold energies for other radionuclidic products that may be produced such as ^{14}O and ^{13}N are 28.9 MeV and 33.5 MeV, respectively, the cross-sections for these reactions are

less than 0.2 mb for energies up to 89 MeV (*18,19*). These low cross-sections should help maintain a relatively radionuclidically pure final product of ^{15}O.

CONCLUSION

Overall, our work illustrates that the production of ^{15}O using a photon-induced nuclear reaction is a promising production method. It may allow for a more straightforward and feasible means of developing ^{15}O onsite for facilities not equipped with a cyclotron.

DISCLOSURE

This research was partially funded by the Indiana University Vice Provost for Research through the Faculty Research Support Program. No other potential conflict of interest relevant to this article was reported.

REFERENCES

1. Van Naemen J, Monclus M, Damhaut P, Luxen A, Goldman S. Production, automatic delivery and bolus injection of [^{15}O]water for positron emission tomography studies. *Nucl Med Biol.* 1996;23:413–416.
2. Inomata T, Fujiwara M, Iida H, Kudomi N, Miura I. Neutron reduction of the small cyclotron for production of oxygen-15-labeled gases. *Int Congr Ser.* 2004;1265:97–100.
3. Mackay DB, Steel CJ, Poole K, et al. Quality assurance for PET gas production using the Cyclone 3D oxygen-15 generator. *Appl Radiat Isot.* 1999;51:403–409.
4. Powell J, O'Neil JP. Production of [^{15}O]water at low-energy proton cyclotrons. *Appl Radiat Isot.* 2006;64:755–759.
5. Harms HJ, Nesterov SV, Han C, et al. Comparison of clinical non-commercial tools for automated quantification of myocardial blood flow using oxygen-15-labelled water PET/CT. *Eur Heart J Cardiovasc Imaging.* 2014;15:431–441.
6. Howard S, Starovoitova VN. Target optimization for the photonuclear production of radioisotopes. *Appl Radiat Isot.* 2015;96:162–167.
7. Mamtimin M, Harmon F, Starovoitova VN. Sc-47 production from titanium targets using electron linacs. *Appl Radiat Isot.* 2015;102:1–4.
8. Talamo A, Gohar Y. Production of medical radioactive isotopes using KIPT electron driven subcritical facility. *Appl Radiat Isot.* 2008;66:577–586.
9. Rane S, Harris JT, Starovoitova VN. ^{47}Ca production for $^{47}Ca/^{47}Sc$ generator system using electron linacs. *Appl Radiat Isot.* 2015;97:188–192.
10. Agostinelli A, Allison J, Amako K, et al. GEANT4: a simulation toolkit. *Nucl Instrum Methods Phys Res A.* 2003;506:250–303.
11. Allison J, Amako K, Apostolakis J, et al. Geant4 developments and applications. *IEEE Trans Nucl Sci.* 2006;53:270–277.
12. Allison J, Amako K, Apostolakis J, et al. Recent developments in Geant4. *Nucl Instrum Methods Phys Res A.* 2016;835:186–225.
13. Bramblett RL, Caldwell JT, Harvey RR, Fultz SC. Photoneutron cross sections of Tb^{159} and O^{16}. *Phys Rev.* 1964;133:B869–B873.
14. Caldwell JT, Bramblett RL, Berman BL, Harvey RR, Fultz SC. Cross sections for the ground- and excited-state neutron groups in the reaction $O^{16}(y, n)^{15}O$. *Phys Rev Lett.* 1965;15:976–979.
15. Peeples JL, Stokely MH, Michael Doster J. Thermal performance of batch boiling water targets for ^{18}F production. *Appl Radiat Isot.* 2011;69:1349–1354.
16. Peeples JL, Stokely MH, Poorman MC, Bida GT, Wieland BW. Simulation, design, and testing of a high power collimator for the RDS-112 cyclotron. *Appl Radiat Isot.* 2015;97:87–92.
17. Williams MC, Mirsadraee S, Dweck MR, et al. Computed tomography myocardial perfusion vs ^{15}O-water positron emission tomography and fractional flow reserve. *Eur Radiol.* 2017;27:1114–1124.
18. Carlos P, Beil H, Bergere R, Berman BL, Lepretre A, Veyssiere A. Photoneutron cross sections for oxygen from 24-133 MeV. *Nucl Phys A.* 1982;378:317–339.
19. Veyssiere A, Beil H, Bergere R, Carlos P, Lepretre A, De Miniac A. A study of the photoneutron contribution to the giant dipole resonance of s-d shell nuclei. *Nucl Phys A.* 1974;227:513–540.